Int. J. Heat Mass Transfer. Vol. 26, No. 7, pp. 1055–1062, 1983
Printed in Great Britain

0017-9310/83 $3.00+0.00

REDUCING SCATTERING TO NONSCATTERING PROBLEMS IN RADIATION HEAT TRANSFER

HAEOK LEE and RICHARD O. BUCKIUS
Department of Mechanical and Industrial Engineering, University of Illinois at Urbana-Champaign, Urbana, IL 61801, U.S.A.

(*Received* 20 *May* 1982 *and in final form* 22 *November* 1982)

Abstract—Radiant heat flux calculations in planar, absorbing, emitting, and isotropic scattering layers are accurately reduced to calculations in nonscattering layers by scaling laws. The two scaling laws, square root and linear, are accurate for different combinations of optical depth and single scattering albedo. The linear scaling applies for the optically thin and the highly scattering problems. The square root scaling is accurate for all others. The heat flux distributions in inhomogeneous, nonisothermal layers which scatter isotropically are obtained by solving multi-layered problems with each layer reduced to a nonscattering problem. Anisotropic scattering effects are easily included.

NOMENCLATURE

e_b, blackbody emissive power, πI_b;
E_3, exponential integral function of order 3;
I, radiation intensity;
T, temperature;
q, radiant heat flux;
q_0, incident radiosity.

Greek symbols
ε, wall emissivity;
κ, optical depth, optical depth coordinate;
κ_0, total optical depth;
μ, $\cos\theta$;
θ, angle with the κ-axis;
ρ, wall reflectivity;
σ, Stefan–Boltzmann constant;
ω, scattering albedo.

Subscripts
E, equivalent quantity;
m, medium property.

Superscripts
$'$, integration variable;
$*$, nondimensional variable;
$^+$, in the positive κ direction;
$^-$, in the negative κ direction.

PROBLEM STATEMENT

THE RADIATION heat transfer calculations for a planar, absorbing, emitting and scattering medium are generally complex. The degree of difficulty in solving the transport equation depends on the nature of scattering. If the medium scatters anisotropically, considerable effort is required to obtain the exact solutions. It has been shown that the radiant heat flux and the average incident radiation in a planar, anisotropically scattering medium can be scaled by an equivalent medium which scatters isotropically [1]. The complexity of the problem is thus greatly reduced, but the governing equation remains in the integro-differential form. The objective of this paper is to show how the governing equation can be reduced to an easily integrable differential equation by scaling all scattering effects into equivalent properties of a nonscattering problem.

There have been attempts at reducing scattering problems to nonscattering problems. Adrianov [2] solved for the net radiant heat transfer between two planar walls at a constant temperature which contain an isothermal, absorbing–scattering gas. The effect of scattering is included in the absorptance of the layer by using the two-flux method. A more generalized scaling technique was introduced by Goswami and Vachon [3]. The two-flux method is also used to calculate the absorptance of an absorbing, emitting and isotropically scattering layer. The resulting absorptance is used to scale the optical depth of the problem to an equivalent length of a nonscattering layer.

For the problem of a cold medium with incident radiosity from the wall located at zero optical depth, the results of the previous scaling attempt are shown in Fig. 1. The exact total heat flux distributions (numerical

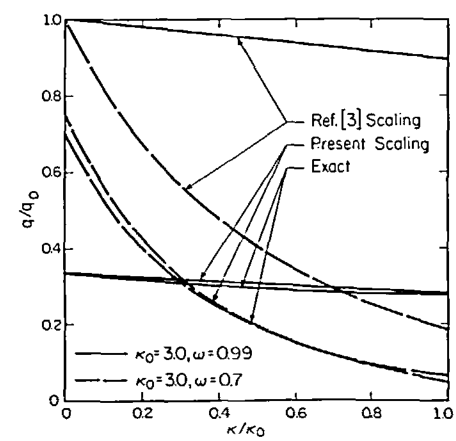

FIG. 1. Heat flux vs optical depth: comparing the previous and the current scaling models.

solution method presented in the Evaluation section) are used to compare the previous scaling results. The scaling approach of Goswami and Vachon, with numerous corrections to the equations as originally stated in ref. [3], is used to generate these results. Although the above scaling attempts to incorporate the effect of scattering, the results are inadequate. Figure 1 shows the results of the scaling scheme which is presented in this work.

The model system under study is a planar isothermal medium at T_m between two diffuse walls with incident radiosity q_0 from the left wall. The medium scatters isotropically while it also emits and absorbs. The equation of transfer is

$$\mu \frac{\partial I(\kappa,\mu)}{\partial \kappa} + I(\kappa,\mu) = (1-\omega)\frac{\sigma T_m^4}{\pi} + \frac{\omega}{2}\int_{-1}^{1} I(\kappa,\mu')\,d\mu' \quad (1)$$

where $I(\kappa,\mu)$ is the radiant intensity, μ is $\cos\theta$ (θ is the angle with the positive κ-axis), κ is the optical depth, ω is the scattering albedo, and σ is the Stefan–Boltzmann constant. The radiant heat flux is obtained by integrating the weighted intensity over μ,

$$q(\kappa) = 2\pi \int_{-1}^{1} I(\kappa,\mu')\mu'\,d\mu'. \quad (2)$$

medium. In a scattering medium, not only is there a decay of energy by absorption there is also a redistribution of energy into all directions. In particular, the net heat fluxes in the positive and the negative κ directions are $q^+(\kappa)$ and $q^-(\kappa)$. The scattering phenomenon yields a significant $q^-(\kappa)$ contribution, called backscattering, which cannot be matched by altering only the emissive characteristics of a nonscattering medium, i.e. by changing the optical depth.

We introduce the effect of backscattering into a nonscattering problem by prescribing an equivalent reflectivity at the wall, ρ_E. The ρ_E of both walls are the same because the heat flux distribution for the system under study (Fig. 2) without boundary terms is symmetric. Since the nonscattering problem where all of the scattering effects are concentrated on the walls must also yield a symmetric heat flux distribution, the equivalent reflectivity of both walls must be identical. The equivalent reflectivity is a function of κ_0 and ω since the magnitude of $q^-(\kappa)$ in the scattering problem is also dependent on these two parameters. The equivalent emissivity is $(1-\rho_E)$.

The details of the scaling are given in the following section. Once the reduction is achieved, the equation of transfer [equation (1)] becomes an easily integrable differential equation. The equivalent heat flux for the problem shown in Fig. 2 is computed simply by

$$q_E(\kappa_E) = 2q_0\left[\frac{(1-\rho_E)E_3(\kappa_E) - 2(1-\rho_E)\rho_E E_3(\kappa_{0_E})E_3(\kappa_{0_E}-\kappa_E)}{1-4\rho_E^2 E_3^2(\kappa_{0_E})}\right] + 2\sigma T_m^4\left\{\frac{(1-\rho_E)[2\rho_E E_3(\kappa_{0_E})+1][E_3(\kappa_{0_E}-\kappa_E)-E_3(\kappa_E)]}{1-4\rho_E^2 E_3^2(\kappa_{0_E})}\right\}, \quad (3)$$

where $E_3(x)$ is the third exponential integral function.

The model problem considered is simple but the above result is fundamental to building solutions of more complicated systems. In the Applications section, we will show how problems with incident radiation from both boundaries (diffuse reflecting walls), nonisothermal or inhomogeneous media can be trivially solved once the problem has been reduced to nonscattering. Effects of anisotropic scattering can also be included by first applying the scaling proposed in ref. [1]. Although the above result is presented for gray properties, the conclusions are also valid on a spectral basis if the spectral blackbody emissive power of the medium is used. We pointed out in ref. [1] that when scaling from anisotropic to isotropic scattering the angular information necessary to scale the intensity field is lost. Thus only the integrated quantities, the heat flux and the average incident radiation, were scaled. In reducing an isotropic scattering problem to a non-scattering problem the directional heat fluxes can no longer be scaled. Thus, only the total radiant heat flux is scaled.

The reduction of the scattering problem to a nonscattering problem is shown schematically in Fig. 2. The incident radiosity q_0 and the temperature of the medium T_m remain invariant under the scaling. The equivalent optical depth κ_E will be scaled to include scattering as well as absorption.

The discussion of Fig. 1 has shown that the resulting equivalent heat flux obtained by scaling only the optical depth is inaccurate. The reason for the error is that the heat transfer characteristics of a nonscattering medium are fundamentally different from a scattering medium.

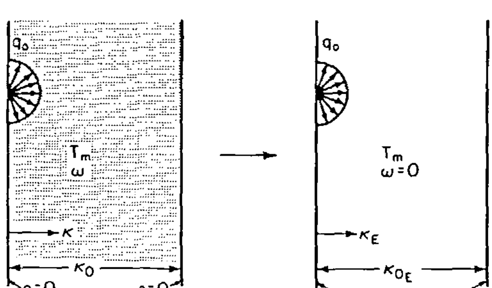

FIG. 2. Physical system model.

SCALING

The P−1 approximation (1st order spherical harmonics approximation) was used to scale anisotropic to isotropic problems [1] and this approximation is the starting point for the present scaling. The governing equation for the isotropic scattering is normalized as

$$\frac{d^2q^*(\kappa^*)}{d\kappa^{*2}} = 3\kappa_0^2(1-\omega)q^*(\kappa^*)+4\kappa_0(1-\omega)\frac{dI_b^*(\kappa^*)}{d\kappa^*} \quad (4)$$

where

$$q^* = \frac{q}{q_0}, \quad I_b^* = \frac{\pi I_b}{q_0} \quad \text{and} \quad \kappa^* = \frac{\kappa}{\kappa_0}.$$

The Marshak boundary conditions are

$$\frac{dq^*(\kappa^*)}{d\kappa^*} - 2\kappa_0(1-\omega)q^*(\kappa^*) = 4\kappa_0(1-\omega)[I_b^*(\kappa^*)-1] \quad \text{at } \kappa^* = 0 \quad (5a)$$

$$\frac{dq^*(\kappa^*)}{d\kappa^*} + 2\kappa_0(1-\omega)q^*(\kappa^*) = 4\kappa_0(1-\omega)I_b^*(\kappa^*) \quad \text{at } \kappa^* = 1. \quad (5b)$$

The scaling groups suggested are $\kappa_0^2(1-\omega)$ and $\kappa_0(1-\omega)$. For an isothermal medium, the governing equation contains only $\kappa_0^2(1-\omega)$ and the group given by the boundary conditions is $\kappa_0(1-\omega)$. Thus, the two possibilities for scaling optical depth are

$$\text{square root: } \kappa_{0_E} = \sqrt{1-\omega}\,\kappa_0, \quad (6a)$$

$$\text{linear: } \kappa_{0_E} = (1-\omega)\kappa_0. \quad (6b)$$

We argued in the previous section that the boundaries must be scaled. Appropriate boundary scaling laws are obtained for the two optical depth scalings. The linear optical depth scaling from the boundary conditions suggests applications to the optically thin systems where the boundary contributions are important. The normalized energy equation for the optically thin limit,

$$\frac{dq^*}{d\kappa^*} = 4\kappa_0(1-\omega)I_b^* - 2\kappa_0(1-\omega)[q^{+*}(0)+q^{-*}(1)] \quad (7)$$

also shows that $\kappa_0(1-\omega)$ is the only scaling group in this limit. Although the model problem with the isothermal medium is not at radiative equilibrium, the temperature distributions for the optically thin problems at radiative equilibrium are nearly isothermal. Therefore, we look to the P−1 solution of a planar medium at radiative equilibrium for a boundary scaling. The heat flux for an absorbing, emitting, isotropically scattering medium with black walls in radiative equilibrium is given by

$$q^* = \frac{1}{\frac{3}{4}\kappa_0+1}. \quad (8a)$$

The equivalent nonscattering problem with the optical depth of κ_{0_E} and the wall reflectivity ρ_E yields the heat flux of

$$q^* = \frac{1}{\frac{3}{4}\kappa_{0_E}+\dfrac{2}{1-\rho_E}-1}. \quad (8b)$$

The similitude between the model and the scaled problem is achieved by setting

$$\rho_E = 1-\frac{2}{\frac{3}{4}(\kappa_0-\kappa_{0_E})+2} \quad (9)$$

where the linear optical depth scaling of equation (6b) is substituted for κ_{0_E}.

The P−1 boundary scaling is expected to become inaccurate as the optical depth increases. At large optical depths, the boundary effects become negligible and the square root is expected to be the appropriate optical depth scaling. Furthermore, the temperature distributions of the radiative equilibrium problems become nonisothermal. A second boundary scaling, which treats isothermal problems, is needed for the optically thick conditions.

The P−1 solution for isothermal media at the optically thick limit as well as a number of two stream approximations were considered [4]. Best results were obtained from the two-flux solution for isothermal media at the optically thick limit. The two-flux boundary scaling is obtained in the following manner. From Tong and Tien [5], we find that the heat flux at $\kappa = 0$ as $\kappa_0 \to \infty$ becomes

$$q(0) = 2(q_0-\sigma T_m^4)\left(1-\frac{1-\sqrt{1-\omega}}{\omega}\right). \quad (10a)$$

The nonscattering solution [equation (3)] as $\kappa_{0_E} \to \infty$ becomes

$$q_E(0) = (q_0-\sigma T_m^4)(1-\rho_E). \quad (10b)$$

The equivalent wall reflectivity is then

$$\rho_E = \frac{2}{\omega}(1-\sqrt{1-\omega})-1. \quad (11)$$

In summary, the two sets of scaling laws are

linear

$$\kappa_{0_E} = (1-\omega)\kappa_0 \quad \text{and} \quad \rho_E = 1-\frac{2}{\dfrac{3\kappa_0\omega}{4}+2}, \quad (12a)$$

square root

$$\kappa_{0_E} = \sqrt{1-\omega}\,\kappa_0 \quad \text{and} \quad \rho_E = \frac{2}{\omega}(1-\sqrt{1-\omega})-1. \quad (12b)$$

The first set of transformations obtained by using the P−1 radiative equilibrium boundary scaling will be referred to as the linear scaling. The second set uses the two-flux optically thick boundary scaling and will be called the square root scaling. The linear scaling is expected to be accurate for optically thin conditions while the square root scaling is expected to be valid as the optical depth increases.

EVALUATION

The two scaling laws of equations (12) are used to scale the heat flux in the scattering problem shown in

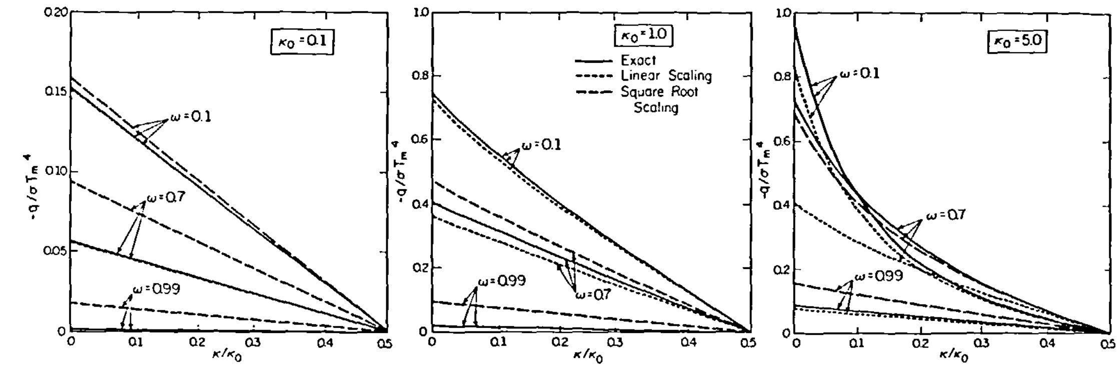

FIG. 3. Heat flux vs optical depth: isothermal emission. (a) Comparison for optically thin limit. (b) Comparison for small optical depths. (c) Comparison for large optical depths.

Fig. 2. These scalings are evaluated by studying (1) isothermal emission with zero boundary temperatures and (2) boundary incidence at $\kappa = 0$ into a cold medium. The equivalent heat fluxes are calculated by equation (3) and compared with the exact solutions. The exact solutions for isotropic scattering are obtained by the adding/doubling approach [6]. The method constructs layer properties from smaller layers where expressions for the reflectance and the transmittance are obtained easily. Internal sources are conveniently included [6, 7]. The results have been shown to be very accurate and computationally fast [6, 7].

From the numerous comparisons done, we present in Figs. 3 and 4 representative results for the cases studied. Figure 3 shows the results for the isothermal emission problems and Fig. 4 is for the boundary incidence problems. Figures 3(a) and (b) and Figs. 4(a) and (b) show that the linear scaling is the better choice for small optical depths. Figures 3(c) and 4(c) show that the linear scaling is also better at very high scattering albedos. Except for these extreme cases, the figures show the square root scaling to be the better scaling. A more precise statement of the regions where each scaling law is applicable is found in Fig. 5.

The scaling regimes shown in Fig. 5 reflect the expected trends, i.e. the linear scaling is better at the optically thin limit and the square root is better at larger optical depths. Figure 5 also shows that the linear scaling is the better scaling method for high albedos, $\omega \to 1.0$. This appears to be a result from the similarity in the heat transfer characteristics of the optically thin medium and the conservative scattering medium, i.e. the heat flux in both cases is a constant.

Figures 3 and 4 are indicative of the magnitudes of error to be expected when the equivalent heat flux results are used. With the correct scaling (Fig. 5), the accuracy is very good for the linear scaling region. In the square root region, the emission problem scales well all the way out to the optically thick limit. The boundary problem in the square root region results in larger error. This is attributable to the error seen from the two-flux boundary solutions. Traugott and Wang [8] show that the heat flux for non-emitting problems is off by 25% and suggest changing a constant of 2 in the governing equation to $3^{1/2}$ to fit the optically thick limit. The suggestion was not followed because it results in emittance values which do not conserve energy. The equivalent heat fluxes for boundary problems do follow the exact distributions at the optically thick limit.

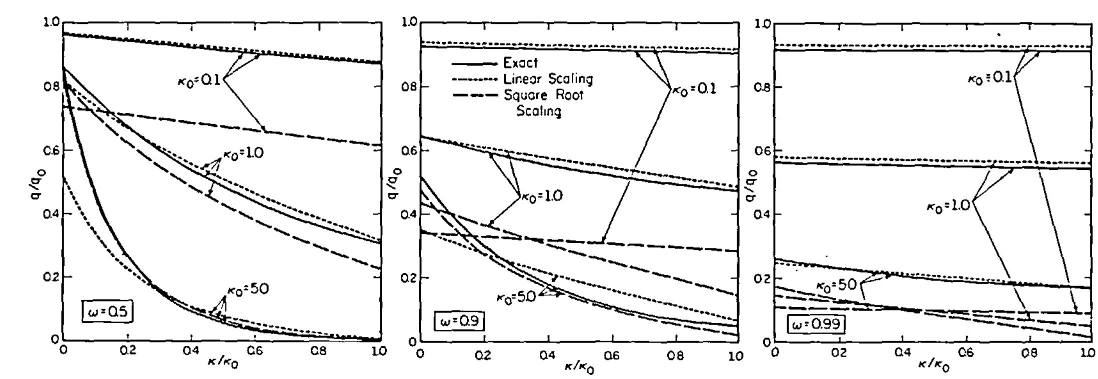

FIG. 4. Heat flux vs optical depth: boundary incidence problems. (a) Comparisons for intermediate scattering albedo. (b) Comparisons for high scattering albedo. (c) Comparisons for cases approaching pure scattering.

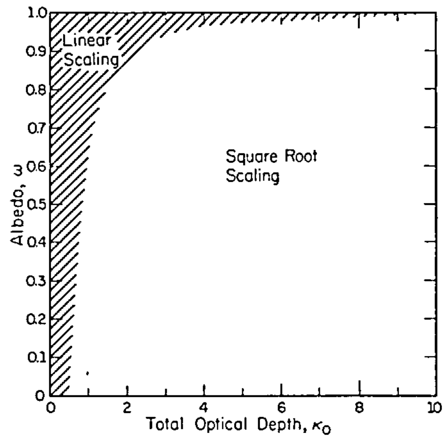

FIG. 5. Scaling regimes.

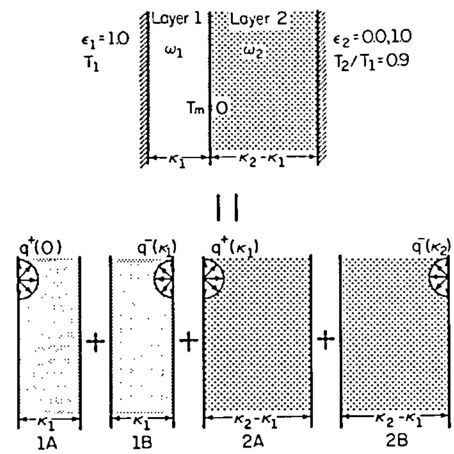

FIG. 6. Inhomogeneous two-layer slab.

Higher errors are seen in the square root region close to the linear region. We will show in the Applications section an approach by which the boundary scaling error in the square root region, especially in the intermediate optical depth region, can be avoided. In addition, the slopes of the equivalent heat fluxes of Figs. 3 and 4 show that the average incident radiation does not scale as well.

APPLICATIONS

Scaling isotropic scattering problems in homogeneous and isothermal media bounded by black walls have been addressed thus far. In general, the temperature of the medium is not uniform and the scattering particles may also be unevenly distributed. The temperature profile of a problem is unknown until the energy equation, which involves other modes of heat transfer, is solved. To solve the radiation part of the problem, the temperature of the medium is needed. The usual approach is to assume a temperature profile for the radiation calculations, use the result in the energy equation, and then iterate.

Given an assumed nonisothermal temperature profile in an inhomogeneous medium, the medium can be subdivided into a number of approximately isothermal layers. We further assume that these sublayers are homogeneous with constant optical properties. Then the isothermal scaling technique presented in the previous sections can be applied directly. In the sample problems presented below, the two effects are separately treated. The problems with diffusely reflecting walls are solved by adding a layer of zero depth to represent the wall. The layers of the medium are scaled without walls and the energy balance on the wall is added to the set of equations to be solved.

To illustrate the solution technique involved in solving inhomogeneous medium problems, a double layered slab is considered. A cold medium is held between two diffusely reflecting walls of different temperatures. As shown in Fig. 6, the heat flux of this problem is treated as a superposition of the heat fluxes from the simpler problems with the boundary sources as indicated. Following the notation shown on Fig. 6, the total heat flux is given by

$$q^*(\kappa) = q^*_{1A}(\kappa) + q^*_{1B}(\kappa)\frac{q^-(\kappa_1)}{q^+(0)}, \quad 0 \leqslant \kappa \leqslant \kappa_1, \quad (13a)$$

$$q^*(\kappa) = q^*_{2A}(\kappa)\frac{q^+(\kappa_1)}{q^+(0)} + q^*_{2B}(\kappa)\frac{q^-(\kappa_2)}{q^+(0)}, \quad \kappa_1 \leqslant \kappa \leqslant \kappa_2. \quad (13b)$$

The * denotes nondimensionalization with respect to $q^+(0)$ and the $q^-(\kappa_1)$, $q^+(\kappa_1)$ and $q^-(\kappa_2)$ are the unknown intermediate and incident radiosities.

These intermediate radiosities need to be explicitly determined when working with single layer solutions whether isotropic or equivalent nonscattering. Assuming that these intermediate radiosities are diffuse, and looking only to conserve directional heat fluxes, the intermediate radiosities are obtained by summing the directional heat fluxes due to each of the sources evaluated at the interface. For the two-layer problem this yields a set of two linear equations. For n-layers, $2n$ simultaneous equations need to be solved. The right side incident radiosity is obtained by an energy balance at the wall, which involves the unknown radiosities. The problem can be formulated in terms of total heat fluxes of the two layers. Each of these heat fluxes can be easily solved by reducing the problem by the appropriate scaling law to a nonscattering problem.

The calculations were done for double layered problems of differing optical properties and ε_2 ranging from 0.1 to 1.0. Of the calculations done, Figs. 7(a) and (b) present the extreme results of $\varepsilon_2 = 0.0$ and $\varepsilon_2 = 1.0$. The agreement between the scaled result using the superposition approximation and the exact solution is excellent. Results were also obtained when the heat fluxes of each layer were calculated by solving the isotropic scattering equations and superimposed. These last results are not presented but they indicate that most of the errors in Fig. 7 are due to the incorrect

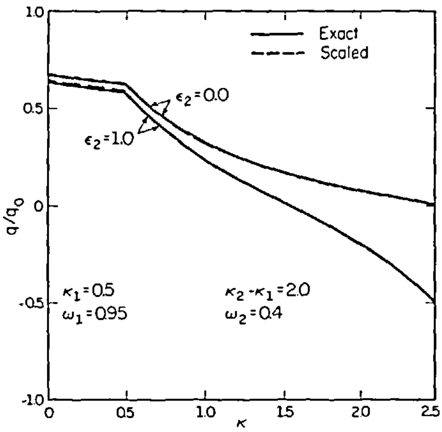

FIG. 7(a). Heat flux distribution for an inhomogeneous double layered slab (see Fig. 5 for scaling regimes).

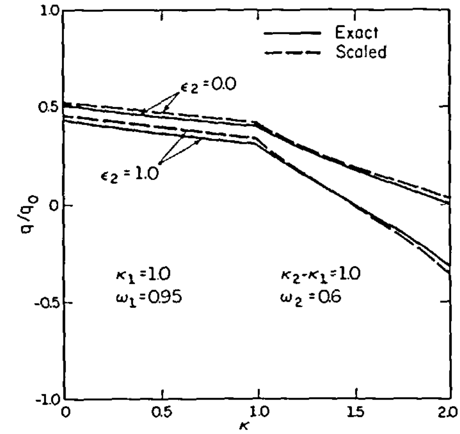

FIG. 7(b). Heat flux distribution for an inhomogeneous double layered slab (see Fig. 5 for scaling regimes).

assumption of diffuse intermediate radiosities and not to the scaling. In the limit of a homogeneous layer having an optical depth which lies in the square root region, subdividing the layer into smaller layers which lie in the linear scaling region usually yields same or better heat flux distributions. The scaling is especially improved for the boundary problems with intermediate optical depths. The interaction between the improved single layer scaling and the error introduced by the diffuse intermediate radiosities assumption is complex and difficult to determine. It does appear that for larger homogeneous layers, say $\kappa_0 = 1.5$, subdividing into a number of linear layers is a desirable approach.

The second effect to demonstrate is the characteristics of a nonisothermal medium. A homogeneous medium is divided into a number of isothermal layers. We will consider a double layered problem shown in Fig. 8. The two layers are identical except for the temperatures. The method of superposition is again used. The total heat flux is given by

$$q^*(\kappa) = q^*_{1A}(\kappa)\frac{q^-(\kappa_1)}{e_{bT_{m1}}} + q^*_{1B}(\kappa), \quad 0 \leqslant \kappa \leqslant \kappa_1, \quad (14a)$$

$$q^*(\kappa) = q^*_{2A}(\kappa)\frac{q^+(\kappa_1)}{e_{bT_{m1}}} + q^*_{2B}(\kappa)\frac{e_{bT_{m2}}}{e_{bT_{m1}}}, \quad \kappa_1 \leqslant \kappa \leqslant \kappa_2, \quad (14b)$$

where * denotes nondimensionalization with respect to $e_{bT_{m1}}$, the emissive power of layer 1. The intermediate radiosities, $q^+(\kappa_1)$ and $q^-(\kappa_1)$ are obtained in the manner described for the first example. The total heat flux distribution is obtained by solving the equivalent nonscattering heat fluxes of problems 1A, 1B, 2A and 2B. Figure 9 shows the plot of the heat flux vs optical depth for $\kappa_1 = \kappa_2 - \kappa_1 = 1.0$ and $\omega_1 = \omega_2 = 0.3$. The equivalent results compare very well with the exact solution.

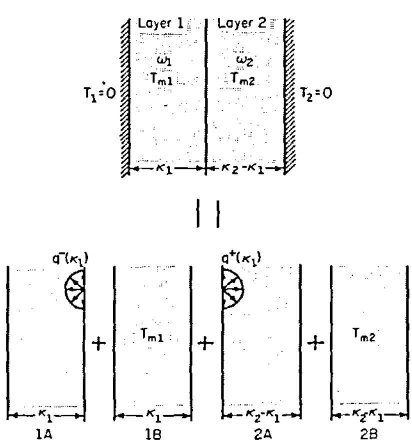

FIG. 8. Nonisothermal two-layer slab.

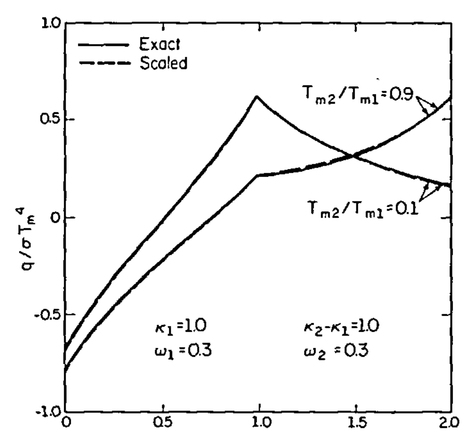

FIG. 9. Heat flux distribution for a nonisothermal double layered slab (see Fig. 5 for scaling regimes).

CONCLUSION

The goal was to reduce the heat flux calculations in scattering problems to that in nonscattering problems. This is achieved by looking at the P – 1 and the two-flux approximations. The scalings obtained are the linear scaling

$$\kappa_{0_E} = (1-\omega)\kappa_0; \quad \rho_E = 1 - \frac{2}{\frac{3}{4}\kappa_0\omega + 2}$$

and the square root scaling,

$$\kappa_{0_E} = \sqrt{1-\omega}\,\kappa_0; \quad \rho_E = \frac{2}{\omega}(1-\sqrt{1-\omega}) - 1.$$

The scaling regimes are presented in Fig. 5. The linear scaling is more accurate for the optically thin and the high scattering albedo problems. The square root scaling is applicable elsewhere. The accuracy in scaling the heat flux in an isothermal medium which scatters isotropically is shown to be excellent. The solution of the simple model problem is fundamental to including inhomogeneous, nonisothermal effects by solving the multi-layered problem. Anisotropic scattering can be included by pre-scaling by the laws given in [1]. Also, all the results are valid on a spectral basis.

Acknowledgement—This work was supported in part by the National Science Foundation under Grant No. MEA-8109250. Mr C. I. Rackmil's efforts in performing the exact numerical calculations are gratefully acknowledged.

REFERENCES

1. H. Lee and R. O. Buckius, Scaling anisotropic scattering in radiation heat transfer for a planar medium, *Trans. Am. Soc. Mech. Engrs*, Series C, ASME, *J. Heat Transfer* **104**, 68–75 (1982).
2. V. N. Adrianov, The role of scattering in radiant heat transfer, *Heat Transfer—Soviet Res.* **1**, 126–132 (1969).
3. D. Y. Goswami and R. I. Vachon, Radiative heat-transfer analysis using an effective absorptivity for absorption, emission and scattering, *Int. J. Heat Mass Transfer* **20**, 1233–1239 (1977).
4. W. E. Meador and W. R. Weaver, Two-stream approximations to radiative transfer in planetary atmospheres: a unified description of existing methods and a new improvement, *J. Atmos. Sci.* **37**, 630–643 (1980).
5. T. W. Tong and C. L. Tien, Resistance-network representation of radiative heat transfer with particulate scattering, *J. Quantve. Spectros. & Radiat. Trans.* **24**, 491–503 (1980).
6. G. N. Plass, G. W. Kattawar and F. E. Catchings, Matrix operator theory of radiative transfer 1: Rayleigh scattering, *Appl. Optics* **12**, 314–329 (1973).
7. W. J. Wiscombe, On initialization, error and flux conservation in the doubling methods, *J. Quantve. Spectros. & Radiat. Trans.* **16**, 637–658 (1976).
8. S. C. Traugott and K. C. Wang, On differential methods for radiant heat transfer, *Int. J. Heat Mass Transfer* **7**, 269–273 (1964).

PROBLEMES DE REDUCTION OU NON DE LA DIFFUSION DANS LE TRANSFERT THERMIQUE RADIATIF

Résumé—Les calculs de flux radiatifs dans les couches planes, absorbantes, émettrices et isotropiquement diffusantes sont réduites à des calculs de couches non diffusantes par des lois d'échelle. Les deux lois d'échelle, racine carrée et linéaire, sont précises pour différentes combinaisons de profondeur optique et d'albedo unique. La méthode linéaire s'applique aux problèmes de couches optiquement minces et fortement diffusantes. La méthode racine carrée convient à tous les autres. Les distributions de flux thermique dans les couches non homogènes et non isothermes qui diffusent isotropiquement sont obtenues en résolvant des problèmes multicouches avec chaque couche réduite à une couche non diffusante. Les effets de diffusion anisotrope sont facilement inclus.

REDUKTION EINES PROBLEMS MIT STREUUNG AUF EIN PROBLEM OHNE STREUUNG BEIM WÄRMEÜBERGANG DURCH STRAHLUNG

Zusammenfassung—Die Berechnung des Wärmeübergangs durch Strahlung in ebenen, absorbierenden, emittierenden, isotrop streuenden Schichten wird durch geeignete Normierung auf die Berechnung von nicht streuenden Schichten zurückgeführt. Die beiden Normierungsgesetze sind quadratisch und linear und lassen sich exakt auf verschiedene Kombinationen von optischer Tiefe und einfach streuendem Albedo anwenden. Die lineare Normierung wird bei Problemen mit optisch dünnen und stark streuenden Schichten angewandt. Für alle anderen Fälle gilt die quadratische Normierung. Die Verteilung der Wärmestromdichten bei inhomogenen, nicht-isothermen, isotrop streuenden Schichten erhält man durch die Lösung von Mehrschichten-Problemen, wobei jede Schicht auf ein nicht-streuendes Problem zurückgeführt wird. Weitere Einflüsse durch nicht-isotrope Streuung können leicht einbezogen werden.

СВЕДЕНИЕ ЗАДАЧ О РАССЕИВАЮЩИХ СРЕДАХ К НЕРАССЕИВАЮЩИМ ПРИ ЛУЧИСТОМ ТЕПЛОПЕРЕНОСЕ

Аннотация—Расчеты лучистого теплового потока в плоских, поглощающих, излучающих и изотропно рассеивающих слоях точно сведены методами подобия к расчетам лучистого теплового потока в нерассеивающих средах. Два закона преобразования, корня квадратного и линейный, позволяют точно рассчитать различные сочетания оптической глубины с одним альбедо рассеяния. Пересчет по линейному закону используется в задачах с оптически тонкими и сильно рассеивающими средами. Пересчет по закону квадратного корня дает точные результаты во всех остальных случаях. Распределение теплового потока в неоднородных, неизотермических, изотропно рассеивающих слоях получено путем решения задач для многослойных сред, в которых для каждого слоя проведен пересчет на нерассеивающую среду. В этом случае легко учитываются эффекты анизотропного рассеяния.